Electronics and Communications in Japan, Part 2, Vol. 90, No. 10, 2007
Translated from Denshi Joho Tsushin Gakkai Ronbunshi, Vol. J89-C, No. 12, December 2006, pp. 1066–1078

Transmission Characteristics of Wireless Baseband Transmission Under Multipath Environments Using Real-Valued Signal Analysis

Jun-ichi Kitagawa, Tetsuki Taniguchi, and Yoshio Karasawa

Advanced Wireless Communication Research Center, The University of Electro-Communications, Chofu, 182-8585 Japan

SUMMARY

Discussed here are real-valued signal analysis and wireless baseband transmission, a system for transmitting baseband signals directly from an antenna, and transmission characteristics under a multipath environment. The field of wireless transmission generally handles band signals in which information rides on a carrier wave, and therefore signal analysis is not the direct analysis of real high-frequency signals (real-valued signals) and is performed with a system expressed using complex numbers, called an equivalent baseband system. However, wireless baseband transmission is based on a transmission system which does not use carrier waves and cannot be handled with an equivalent baseband system. Consequently, it is necessary to have a system of real-valued signal analysis for handling baseband signals, which are real-valued signals, without additional processing. The BER (bit error rate) was used as the standard for evaluating transmission characteristics under a multipath environment of wireless baseband transmission using measured channel characteristics with that algorithm. With a computer, the BER characteristics were found by varying the reflection coefficient, number of delay symbols, the ratio of direct wave power and reflected wave power, and the number of reflected waves. As a result, it was clear that the dominant factor in a multipath environment is the ratio of direct wave power and reflected wave power. © 2007 Wiley Periodicals, Inc. Electron Comm Jpn Pt 2, 90(10): 9–22, 2007; Published online in Wiley InterScience (www.interscience.wiley.com). DOI 10.1002/ecjb.20347

Key words: wireless baseband transmission; real-valued signals; BER; multipath; propagation.

1. Introduction

The object of this paper is to examine the basic transmission characteristics in a multipath environment of wireless baseband transmission [1] using real-valued signal analysis. Wireless baseband transmission, unlike earlier wireless transmission systems, uses an antenna to transmit a baseband signal which is the information signal itself [2]. This is a new wireless transmission system which is unlike the present-day general concept of wireless transmission and can be regarded as the application of baseband transmission, which is used in wired transmission, to wireless transmission. A consideration of sine waves which are used as carrier waves in conventional wireless transmission gives one the image of information riding on each wave; this is the ultimate wireless transmission system which could make possible ultrahigh-speed transmission. The application of this technology will make it possible to seamlessly connect wired and wireless transmission systems, realizing high-capacity, high-speed wireless transmission with essential high-speed transmission characteristics.

One wireless system on which attention has been focused in recent years is ultrawide band (UWB) [3–7]. UWB is also called an ultra-wideband wireless system and has the width of the fractional bandwidth in common with this wireless baseband system. However, UWB still includes the operation of modulation which is widely used in general wireless systems including pulse modulation, while the concept of modulation is not part of wireless baseband transmission.

The authors mainly examine the fundamental characteristics of the system itself rather than earlier, specific applications of wireless baseband transmission. In consideration of future deployment, the following two points are considered to be significant for applications. The first is the lack of development of the millimeter wave and terahertz domain, or the exploitation of nearby domains. This is because wireless baseband transmission is a wireless system with a very large fractional bandwidth and such a wireless system will be accepted in areas where interference with other wireless systems is comparatively low. The millimeter wave and terahertz domains are promising candidates. The second is application to short-distance communications (near-field communications) with weak radio waves. This is relevant to micrometer-order wireless transmission for communications between micromachines and chips. Based on earlier assumptions, it was difficult to consider wireless transmission at micrometer-level distances, and it was conceivable that a new wireless transmission system would be required. In addition, use in underground spaces and spaces with metal partitions, where the problem of interference can be ignored, is also considered.

As a concrete examination of wireless baseband transmission, an experiment was performed in a free space environment where the presence of reflected waves, which have normally been problematic for wireless transmission before now, can be ignored. As a result, it was made clear experimentally that wireless baseband transmission was possible with appropriate selection of the transmission path encoding and antenna [1]. The authors used Manchester encoding and a discone antenna, which have been mainly used before now, as the line coding and antenna. In order to make wireless baseband transmission more practical, it is also necessary to evaluate the characteristics in a multipath environment where reflected waves are present. Before now, a large amount of research has been performed regarding transmission characteristics in a multipath environment for general wireless communication [8]. A number of channel models have also been disclosed for UWB [9], but these have not been sufficiently researched. Transmission characteristics in a multipath environment have not yet been completely studied for wireless baseband transmission. The characteristics need to be evaluated in a multipath environment, as well as in free space as in the past, in order for a comprehensive understanding of the performance of a wireless system. In wireless baseband transmission as well, qualitative prediction of the deterioration of transmission characteristics in a multipath environment can be an easy matter. However, in order to have a more complete transmission system, it is necessary to find the deterioration characteristics as specific numerical values. The bit error rate (BER) is used as the benchmark in this paper. It is also necessary to make an evaluation from the perspective of the degree to which a multipath environment will be practical. Accordingly, in this paper, a multipath received waveform was generated on a computer using channel characteristics measured in order to examine the deterioration characteristics for a multipath environment, and the BER characteristics were found.

This paper is structured as follows. In Section 2, the theory of transmission of real-valued signals as an analysis method for baseband signals, the BER calculation method, and the validity of the analysis method in this paper are discussed. Regarding the analysis of wireless baseband transmission, the necessity of treating these all as real systems is discussed and these differ with regards to the possibility of analysis with an equivalent baseband system (expressing signals as complex numbers) in conventional wireless transmission. Section 3 shows the measurement of propagation characteristics using a vector network analyzer (VNA), along with the channel characteristics and impulse response. In Section 4, the BER characteristics calculated using the measured channel characteristics, the BER characteristics when the reflection coefficient is varied, the BER characteristics relative to the ratio of the direct wave power and reflected wave power, and the BER characteristics when varying the number of reflected waves are shown. Discussions are made and conclusions are given in Section 5.

2. Analysis of Baseband Signals

In general, the representation of signals in wireless transmission using sine waves as carrier waves does not use a band system with a real high-frequency signal shown without modification; instead, the signals are represented with a system called an equivalent baseband system using a complex envelope (complex baseband system signal). The fractional bandwidth of the wireless system is at most several percent. In a general sense, this is an information signal riding on a carrier wave rather than the behavior of the carrier wave itself. Therefore, an analysis which includes even the carrier wave is very wasteful because of the very large frequency range which must be expressed. Consequently, analysis with an equivalent baseband system has a reduced computational cost and is said to be efficient.

However, when the case of wireless baseband transmission is considered, there is no concept of a carrier wave and treatment with an equivalent baseband system is not possible. It is necessary to handle real signals in their unaltered state in the same manner as a band system in general wireless transmission. In other words, signals will be analyzed as real-valued signals.

2.1. Real-valued signal transmission theory

The treatment of real-valued signals is discussed with time domain and frequency domain representations. Moreover, in this paper, the system is regarded as being linear and time invariant.

2.1.1. Time domain representation

The relationship of transmitted and received signals in a linear time-invariant system is expressed as follows where the transmitted signal is $s(t)$, the impulse response of the system is $h(\tau)$, and the noise (additive) is $n(t)$; thus, the received signal $r(t)$ becomes

$$\begin{aligned} r(t) &= \int_{-\infty}^{\infty} h(t-\tau)s(\tau)d\tau + n(t) \\ &= h(t) \otimes s(t) + n(t) \end{aligned} \quad (1)$$

Here, τ denotes the delay and $\otimes$ denotes the convolution integral. These quantities are all real.

2.1.2. Frequency domain representation

The following is a result of considering the frequency domain in the same manner as in Section 2.1.1.

$$\begin{aligned} R(f) &= H(f)S(f) + N(f) \\ &= \{H^+(f)S^+(f) + N^+(f)\} \\ &\quad + \{H^-(f)S^-(f) + N^-(f)\} \end{aligned} \quad (2)$$

Here, $R(f)$, $H(f)$, $S(f)$, and $N(f)$ are respectively the Fourier transforms of the $r(t)$, $h(t)$, $s(t)$, and $n(t)$ components. The + and – superscripts denote positive and negative frequency components. The concept of positive and negative frequencies must be considered in the case of the Fourier transforms of real-valued signals.

2.1.3. Real-valued signals and analytical signals

$r(t)$, $s(t)$, and $n(t)$ on the one hand and $R(f)$, $S(f)$, and $N(f)$ on the other are respectively generalized as $x(t)$ and $X(f)$. $x(t)$ is a real-valued signal [in a general analysis, it is not necessary to limit $x(t)$ to a real-valued signal, but it is treated as a real-valued signal in this paper]. Let the analytical signal be $a(t)$; then $a(t)$ is defined as a complex signal comprising the doubled positive frequency component of the $x(t)$ spectrum, and the real part is equal to the real-valued signal which is the original signal. Specifically,

$$a(t) = 2\int_0^{\infty} X(f)e^{j2\pi ft}df = x(t) + j\hat{x}(t) \quad (3)$$

and then is expressed as follows:

$$\mathrm{Re}\,[a(t)] = x(t) \quad (4)$$

Here, the coefficient 2 on the first right-hand side of Eq. (3) is to satisfy Eq. (4); the hat in the second term on the right-hand side of Eq. (3) denotes the Hilbert transform. Re[] in Eq. (4) indicates the real part. In the case of a real-valued signal, $X^+(f)$ and $X^-(f)$ have a complex conjugate relationship; whichever component is found, the other can also be found. The data which can be captured by the VNA used in this experiment can be regarded as corresponding to $X^+(f)$; thus, in the case of this paper, it is necessary to add the data for the negative frequency component afterwards.

2.2. BER calculation

2.2.1. Measurement and simulation

In order to evaluate transmission characteristics with BER, the authors considered making actual measurements, and also developing an appropriate model and performing a computer simulation. It is difficult to construct instruments to measure the BER of a wireless baseband transmission system. Simulation is easy compared to measurement. However, the treatment of the multipath propagation portion for wireless baseband transmission is problematic (Fig. 1). In this paper, therefore, measured data for channel characteristics (complex numbers) only were captured using the VNA; the problem described above was resolved by performing other processing on a computer.

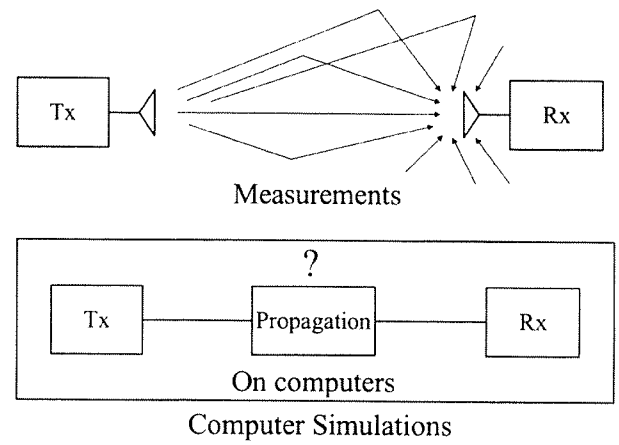

Fig. 1. Measurements and computer simulations.

2.2.2. Processing algorithm

Figure 2 shows an overview of the processing method for BER calculation. The difference from finding the BER through a general wireless communications simulation is that the signals in the time domain are all treated as real numbers. Figure 2 is described below for the discussion of the BER characteristics calculations shown in Section 4.

2.2.3. Signal generation

The data stream to be the transmitted signal is generated using a computer. Manchester encoding is employed for the data stream in this paper. In Manchester encoding, the information is contained in transitions of the values rather than the values themselves. There are two ways of determining the values: for a transition from 1 to 0, 1 corresponds to 10 or, oppositely, 01. This paper uses positive logic, which is the former case of 1 becoming 10 (and 0 becoming 01). A single data stream can include any number of bits, but in this paper will include 200 bits based on the relationship of the number of samples on the time axis. It is confirmed that Manchester encoding is superior in showing BER characteristics in wireless baseband transmission, compared to NRZ (non-return-to-zero) and RZ (return-to-zero) encoding which are widely used in the field of data communications [1]. However, the transmission rate becomes half that of NRZ.

2.2.4. Multiplication by channel characteristics captured with VNA

The prepared data stream underwent FFT (fast Fourier transformation) and was multiplied by the channel characteristics data captured with VNA. At this time, as shown in Fig. 2, a complex conjugate is appended to the end of the VNA-captured data in order to make possible multiplication of the FFT data stream (real-valued signal). In this paper, the number of VNA captured data is 801 as discussed in Section 3.2; a complex conjugate is appended to this as a negative frequency component, but in consideration of FFT symmetry, the total number of data becomes 1600, because the data component corresponding to direct current (300 kHz in this experiment) and the Nyquist frequency (8 GHz in this experiment) component need to be excluded.

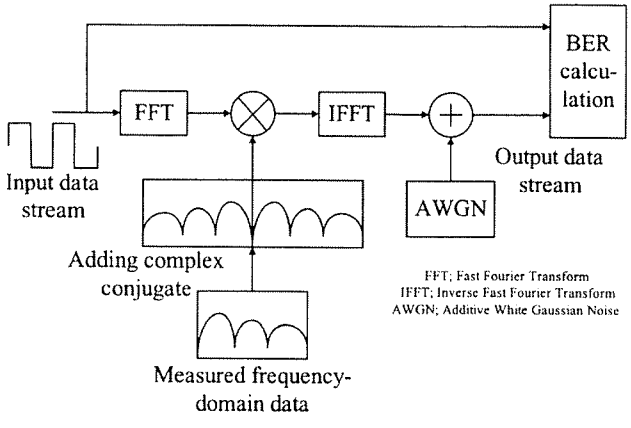

Fig. 2. Procedure of BER calculation (block-by-block processing where each block contains 200-bit with 1600 sampled data).

2.2.5. BER calculation

After the data stream and channel characteristics are multiplied in the frequency domain, IFFT (inverse fast Fourier transformation) is performed, the data are returned to the time domain, and this becomes the received signal. At this time, the received signal power which is necessary for calculating BER characteristics is also found. Furthermore, the received data are distinguished as those which are ideally synchronized with the received signal and compared with the transmitted data, and the number of bit errors is found. At this time, additive white Gaussian noise is added. To assure a BER value of 10^{-5}, the number of transmitted bits must be 10^6 or more. In the case of this paper, 200 bits are transmitted in a single trial, and therefore the number of necessary bits to find the BER is ensured by repeating this 10^4 times (200 times 104 bits). As a result, the BER is found for a single E_b/N_0 (energy to noise power density per bit) value and this is repeated the number of times necessary to ascertain the BER characteristics. In this paper, the BER is found for 16 values of E_b/N_0 in 2-dB steps from 0 to 30 dB.

2.3. Validity of the method of analysis

2.3.1. Uniformity of the time domain and frequency domain measurements

In this paper, the BER characteristics are evaluated using channel characteristics in the frequency domain measured with the VNA, which is different from time domain measurement using a BER tester or oscilloscope performed in general wireless communications, or complete time domain simulation. The following condition is necessary in order to prove the validity of this method. Specifically, channel characteristics captured with the VNA and transmitted data generated by a computer are multiplied in the frequency domain after FFT; then a time domain waveform obtained by performing IFFT matches a real waveform measured directly in the time domain using a signal generator and an oscilloscope. This issue is confirmed in Ref. 1, and Fig. 3 shows an example pulled from the reference of a waveform obtained by both methods in order to show the validity of the analysis. Figure 3(a) shows the transmitted signal generated by the signal generator.

Because this is in Manchester encoding, the information is expressed as {100010011010111}. Figures 3(b) shows the received waveform (solid line) measured with the oscilloscope and a waveform (dotted line) obtained by computer processing after capture with the VNA of only the channel characteristics. Moreover, the type of antenna in Ref. 1 used to obtain the results in Fig. 3 is the discone antenna used in this paper as well, but the size is different from that used in this paper and has a minimum design frequency of 100 MHz. This is from venturing to manufacture a large-sized antenna, making possible the direct measurement of waveforms with an oscilloscope with a 500-MHz bandwidth [1]. Compared to the waveform in Fig. 3(b), both the waveform directly measured with the oscilloscope and the waveform obtained from the VNA and the computer were confirmed to be slightly shifted relative to the amplitude. This is believed to be an effect of instrument error from the oscilloscope and the VNA. However, slippage in the time axis direction was almost totally unconfirmed and because there was no great slippage of the amplitudes, it is believed that there is no problem with inputting results measured with the VNA to the computer and calculating the transmission waveform.

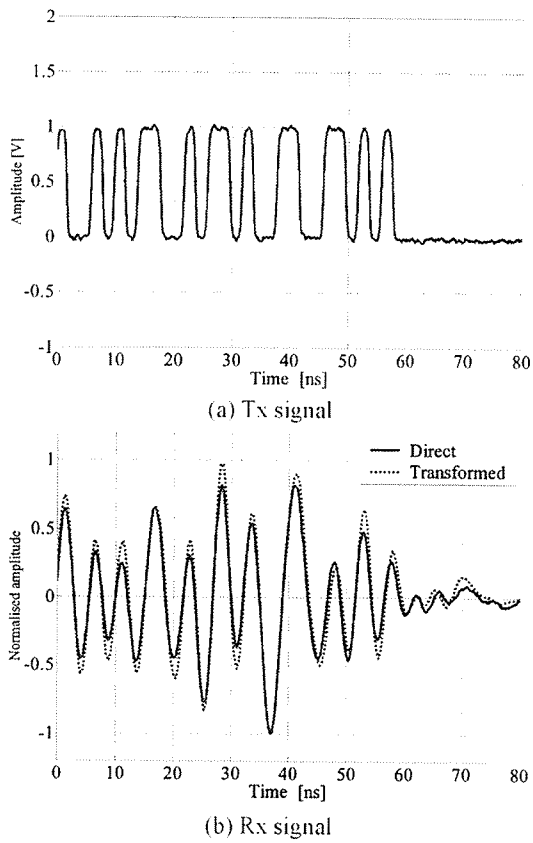

Fig. 3. Direct measured waveform and transformed waveform from frequency domain.

2.3.2. Multipath received waveform generation from channel characteristics data

In this paper, measurement was performed in a shield room as discussed in Section 3, and therefore a multipath environment was created inside the shield room. The multipath environment itself can easily be prepared by establishing a body to reflect radio waves appropriately inside the shield room. However, there is an infinite number of combinations of the placement and number of reflective bodies. Considering the amount of work involved in placing the reflective bodies and making measurements even in an environment which is thought to show representative characteristics, it is not efficient to actually place reflective bodies inside a shield room and take measurement after measurement. Therefore, the authors considered generating a multipath received waveform adjustably on a computer using the channel characteristics measured with the VNA. Specifically, this is a method for generating a multipath waveform as follows: channel characteristics, in a free space (no reflective bodies) state in a shield room were measured with the VNA; those channel characteristics were input to a computer, multiplied with received data prepared on a computer and which underwent FFT, and were then returned to the time domain with IFFT to generate a received waveform in a free space; and reflected waves were synthesized for that waveform with consideration of an arbitrary reflection coefficient and propagation loss. Figure 4 shows the validity of the analysis method. Specifically, as shown in Section 3.3, this is (1) the free space state [Fig. 7(a)] in the shield room, (2) one reflection board placed 1 meter from the transmitting and receiving antennas (1 m) and parallel to the transmitting and receiving antenna direction [path difference of the direct wave and reflected wave $\Delta d = 1.2$ m; Fig. 7(b)], and (3) a waveform synthesized from a waveform relative to the direct wave obtained from (1) on a computer and a reflected wave generated by multiplying that waveform with the reflection coefficient and delaying it. (2) and (3) [Fig. 4(c)] are shown to agree well. Figure 4(a) shows {100010011010111} as the information because of Manchester encoding as in Section 2.3.1. Here, when the waveform (3) is $y(t)$, waveform (1) [Fig. 4(b)] is obtained by multiplying the following as $x(t)$ on a computer:

$$y(t) = x(t) - 0.45x(t - \tau) \qquad (5)$$

The negative sign on the second term on the right-hand side is because the reflection coefficient is treated as -1 (real number); the coefficient 0.45 is due to the propagation loss of the reflected wave; and $\tau = 4.0$ ns. As discussed in Section 2.3.1 and this section, the analysis method in this paper can be said to be valid.

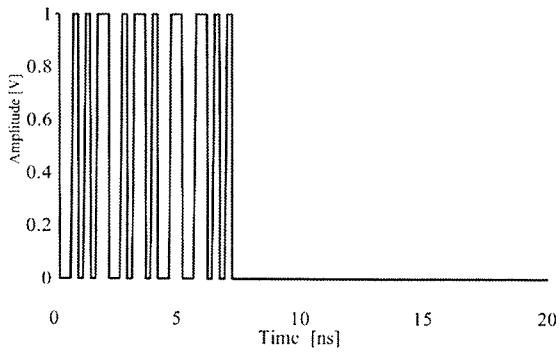

(a) Transmitted waveform

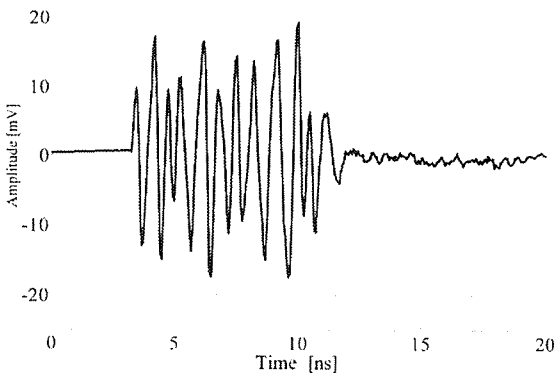

(b) Received waveform (Free space)

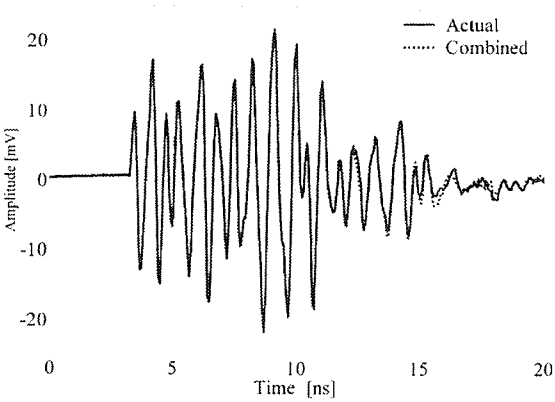

(c) Received waveform (Multipath, $\Delta d = 1.2$ m)

Fig. 4. Received waveforms: reflection board is set up actually (solid line) versus combined waveform on computers (dotted line).

3. Measurement of Propagation Characteristics

3.1. Antenna characteristics

Wireless baseband transmission requires an ultrabroad bandwidth, and the antenna becomes a very important device. Here, the authors used a discone antenna determined to be sufficiently practical for wireless baseband transmission based on prior experimental results [1]. Figure 5 shows the 10-cm discone antenna used for the measurements and also for transmission and reception. The minimum frequency was designed to be 1 GHz and the antenna was made by forming copper panels. Considering the antennas will be placed in a shield room, frequencies near the microwave range are appropriate so that the antennas can be made small. However, there must also be a broad range of measured data because of the following: (a) the VNA measurable range of 300 kHz to 8 GHz, (b) antenna finishing precision, (c) amplitude (dampening) characteristics and phase characteristics of the power supply cable, and (d) wireless baseband transmission requiring broad bandwidths. Moreover, when the minimum frequency of the antenna is near the upper end of the VNA measurable range, the frequency cannot be raised immoderately in view of the idea that significant data cannot be captured in some cases (for example, when the minimum frequency of the antenna is 7 GHz, then data from 300 kHz to 7 GHz, from among data in the measurable range of 300 kHz to 8 GHz,

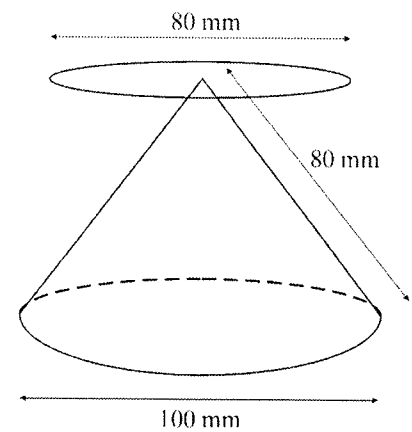

material: copper

(a) Dimensions

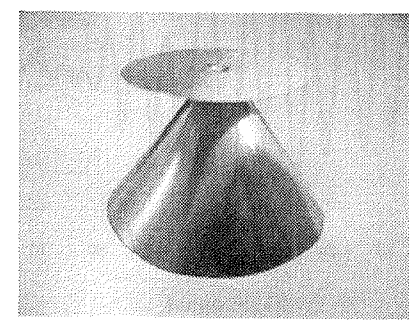

(b) View

Fig. 5. Designed discone antenna.

will be data occurring where the antenna does not function). Consequently, in this paper, the minimum frequency was set at 1 GHz in consideration of the above points (a) to (d). Figure 6 shows the VSWR (voltage standing wave ratio) of the discone antenna (Fig. 5) used in the experiment. From Fig. 6 it can be determined that the VSWR is suppressed to below 2 in the 1 to 6 GHz range and operation in this range is good.

3.2. Measurement with the network analyzer

There are two types of high-frequency network analyzer: the scalar type and vector type. Because the vector type is used in this research, the S (scattering) parameter is measurable and the measured data become complex data in the frequency domain. Furthermore, these data can be regarded as corresponding to the positive frequency component when the Fourier transform is considered to be used, as discussed in Section 2.1.3. Meanwhile, the baseband signal, which is the information signal, is a real-valued signal and has positive and negative frequency components. Consequently, it is not possible to directly calculate the Fourier transform of the VNA measured data (channel characteristics) which do not have a negative frequency component and the baseband signal which has both components. In this paper, therefore, a complex conjugate signal, which is the negative frequency component, is added to the VNA measured data to create a real-valued signal and then the calculations are performed (Fig. 2). As a result, for the Fourier transform of the VNA measured data and baseband signal, both the positive and negative frequency components have a complex conjugate relationship and take real values in the time domain.

S_{21}, where the transmission antenna is 1 and the reception antenna is 2, is captured as the channel characteristics for the BER calculation; this is input to a computer and calculations are performed. There are 801 points of captured data (S_{11}, S_{21}, S_{12}, S_{22}) in the range of 300 kHz to 8 GHz (at about 10-MHz intervals). The premeasurement calibration is two-port full calibration.

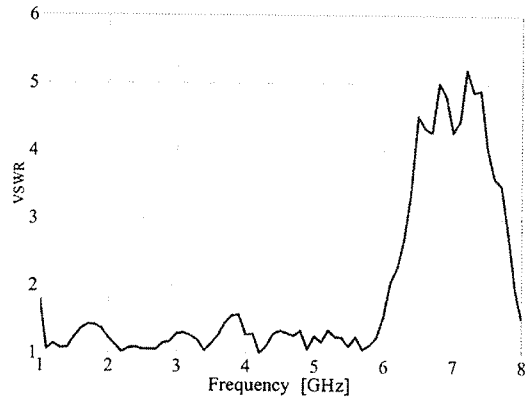

Fig. 6. VSWR characteristic of the discone antenna.

3.3. Measurement environment

Figure 7 shows the measurement environment seen from above. As shown in Fig. 7, the measurements are all performed with reflection boards placed in our university's shield room. The reflection boards comprise 1.8-m-tall, 0.90-m-wide polystyrene foam boards covered with aluminum foil and these are placed vertically. Two sets of measurements were made with (a) no reflection boards and (b) horizontal reflection boards. The path difference for the direct waves and reflected waves in the (b) case was 1.2 m for a time difference of 4.0 ns. The height of the transmission and reception antennas was 1.5 m.

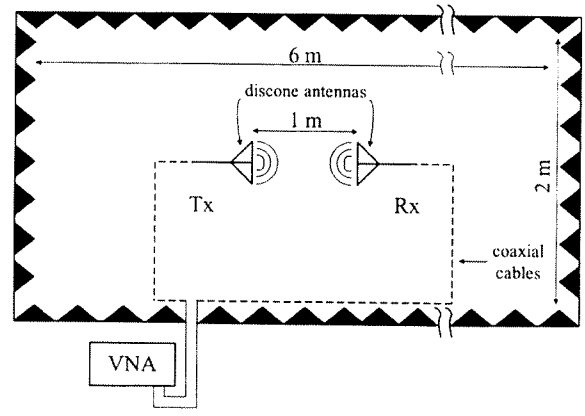

(a) No reflection boards

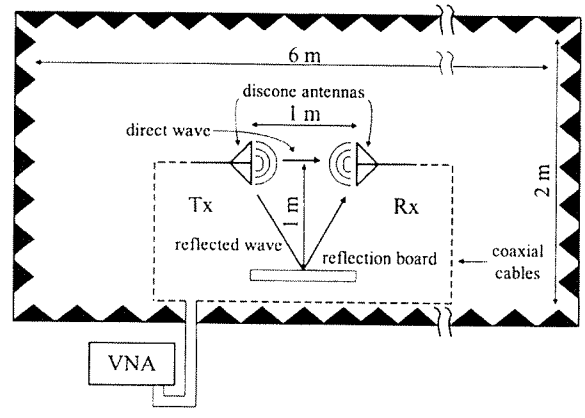

(b) One reflection board

Fig. 7. Measurement environments (upper view).

3.4. Channel characteristics

Figure 8 shows the channel characteristics (S_{21}) captured with the VNA. The indicated frequency range in Fig. 8 is 1 to 6 GHz in consideration of Section 3.1. Figure 8(a) shows the characteristics in free space and the characteristics of –6 dB/octave [1]. The deviation of the measured values from the –6 dB/octave characteristics from near 4 GHz is believed to be a result of the disarrangement of the vertical orientation of the discone antennas as the frequency rises. Figure 8(b) shows that the presence of the reflection board produces ripple in the channel characteristics. The period of the ripple becomes 250 MHz, the inverse of 4.0 ns which is the delay time difference of the direct wave and reflected wave. In fact, Fig. 8(b) also shows such characteristics (for example, there are four nulls between 2 and 3 GHz).

The observation of the impulse response of the channel characteristics is given as another method for understanding the multipath situation. Figure 9 shows the IFFT results of the channel characteristics in Fig. 8 captured with the VNA. Figure 9(a) shows the free space case; it is understood that the response is delayed by the time (3.3 ns) for propagation over the 1 m distance between the transmitting and receiving antennas. The weak reflected wave near 10 to 11 ns in Fig. 9(a) is a multiple reflection between the transmitting and receiving antennas due to the frequency component in excess of the frequency range matching the antennas. Specifically, radio waves from the transmitting antenna take 3.3 ns to arrive at the receiving antenna, but the frequency component which does not match one part of the antennas is reflected (rebroadcast) by the receiving antenna and returned through the space toward the transmitting antenna where it is reflected again and travels to the receiving antenna. The difference in distance with the direct wave at this time is about 2 m and the time difference is about 7.0 ns. The response understandably takes about 10 to 11 ns. In the case of Fig. 9(b) where the reflected wave is present, the time difference between the direct wave and the reflected wave is 4.0 ns as discussed in Section 3.3 and therefore, the response of the reflected wave appears delayed by that amount from the direct wave.

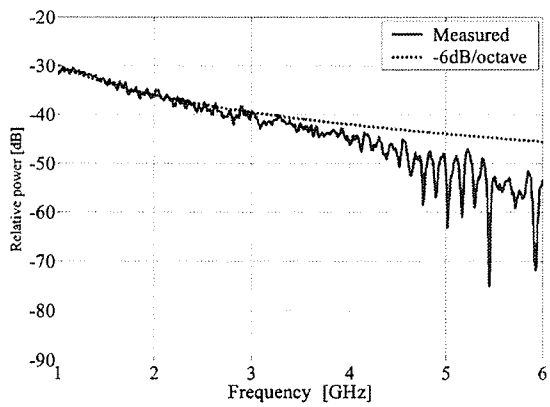

(a) No reflection boards

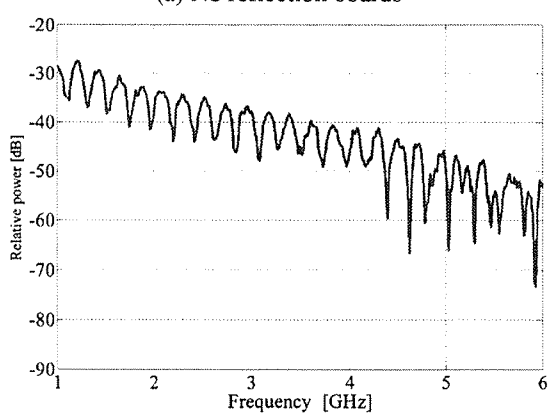

(b) One reflection board

Fig. 8. Channel characteristics.

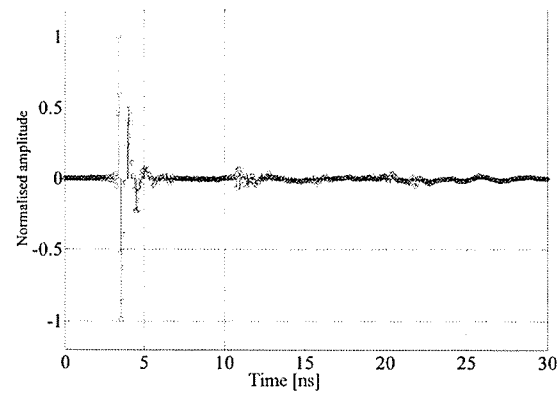

(a) No reflection boards

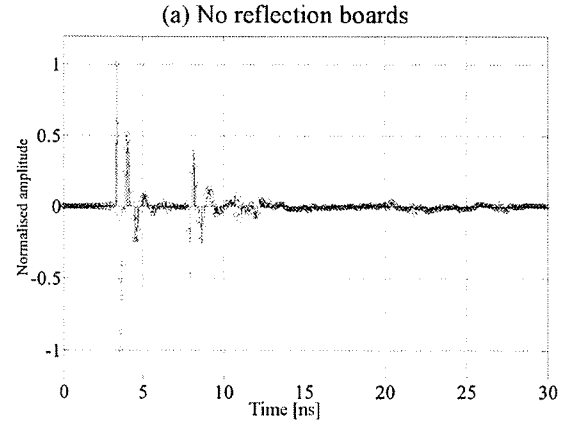

(b) One reflection board

Fig. 9. Channel impulse responses.

4. Evaluation of Transmission Characteristics

4.1. BER characteristics in the measurement environment

Figure 10 shows the BER characteristics for the channel characteristics measured in the environment shown in Fig. 7. As the horizontal axis E_b/N_0 in Fig. 10, the E_b/N_0 for all direct waves (not direct wave + reflected wave) is considered in this paper. The multipath results are expressed with the following: the BER ("actual" in Fig. 10) for the measured channel characteristics acquired in a multipath environment with a real reflection board as discussed in Section 2.3.2, and the BER ("combined" in Fig. 10) for multipath received waveform synthesized on a computer using the measured channel characteristics acquired in free space. The BERs found with both methods agree well as understood from Fig. 10, and Fig. 10 indicates that there is no problem with generating a multipath environment on a computer from the measured channel characteristics of the direct wave component. Manchester encoding as discussed in Section 2.2.2 was used for the data transmission in the process of creating Fig. 10. The minimum unit pulse width composing the waveform is 0.2 ns in consideration of the relationship to the antenna bandwidth obtained in Ref. 1. At this time, because Manchester encoding is employed, the symbol length becomes 0.4 ns and the transmission rate becomes its inverse, 2.5 Gbit/s. In Fig. 10, good transmission in the case of free space can be expected even without the occurrence of an error floor, but in the multipath environment established here, an error floor is generated and the BER falls slightly short of 10^{-3}. This state is considered to be the practical limit of combining channel equalization and error correction technology in actual communications. The delay time of the reflected wave is 4.0 ns as discussed in Section 3.3; therefore, a reflected wave with a delay of 10 symbols arrives and it can be understood that the influence of symbol interference is connected to the occurrence of the floor. Also, in Fig. 10, for comparison with general wireless transmission, the theoretical value of the error rate P_b in synchronous detection of BPSK (binary phase shift keying) for the AWGN (additive white Gaussian noise) transmission path is expressed as follows.

$$P_b = \frac{1}{2}\mathrm{erfc}\sqrt{E_b/N_0} \tag{6}$$

However, E_b/N_0 in Eq. (6) is a true value; erfc expresses the complementary error function. In a comparison of BPSK and wireless baseband transmission, E_b/N_0 is slightly less than 3 dB where BER is 10^{-4}, but becomes all the more necessary in wireless baseband transmission. However, in performing 2.5-Gbps transmission using BPSK from a conventional perspective, a 250-GHz propagation wave is necessary when the fractional bandwidth is 1%. This is difficult, considering the equipment and antenna for this purpose. Consequently, although E_b/N_0 which is more important for wireless baseband transmission than BPSK often becomes about 3 dB (in the case of this paper), it is possible to realize a wireless transmission system (gigabit transmission using gigahertz waves) suitable for high-speed, high-capacity transmission.

4.2. BER characteristics resulting from changes to the reflection coefficient

Figure 11 shows the BER characteristics in the case where the reflection coefficient γ is varied from –1 [multipath in Fig. 10 (combined)], –0.8, –0.5, –0.2, 0 [free space in Fig. 10 (actual)] where the reflected wave arrives with a 10-sample delay (path difference 1.2 m) as in Section 4.1.

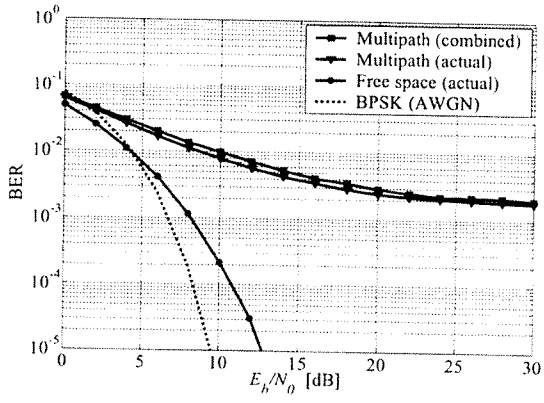

Fig. 10. BER characteristics under the measurement environment.

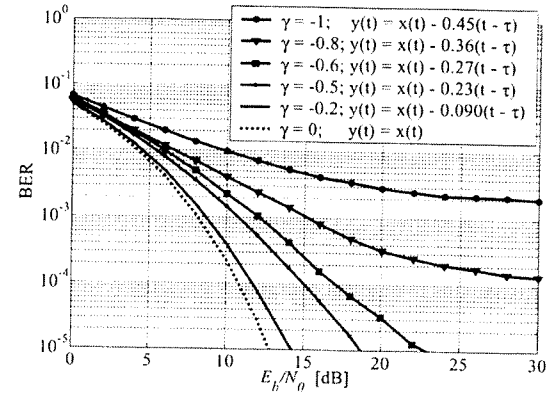

Fig. 11. BER characteristics with varying γ [reflection wave arrives with 10-symbol delay (τ = 4.0 ns) of direct wave].

The legend of Fig. 11 lists the numerical values of the received waveforms generated on a computer in the same manner as in Eq. (5). From Fig. 7(b), the floors occur with the BERs in the vicinity of 10^{-3} and 10^{-4} respectively for the cases $\gamma = -1$ and $\gamma = -0.8$. In the other cases, a floor is not generated and transmission is shown to be possible even in a multipath environment. The values of the BER floors are considered here. In the case of $\gamma = -1$, the BER floor is 10^{-3}. In this case, when the reflected wave is regarded as an interference (unnecessary) component as seen from the direct wave, the *S/I* (signal-to-interference ratio) from Eq. (5) becomes approximately 7 dB. Compared to the value of E_b/N_0 = 7 dB of free space (actual) in Fig. 10 where the interference component *I* is regarded as noise, this *S/I* becomes a value in the vicinity of 10^{-3} which is identical to the BER floor value at $\gamma = -1$. Likewise, in the case of $\gamma = -0.8$, the *S/I* = 9 dB; the value of E_b/N_0 = 9 dB in free space (actual) in Fig. 10 becomes a value in the vicinity of 10^{-4} which is the BER floor value where $\gamma = -0.8$. Also, overall good characteristics were displayed as the reflection coefficient approached zero (reflected wave becoming weak), and these results are said to be valid.

In this section, to examine the influence of the reflected wave on BER characteristics, the reflection coefficient was varied and the characteristics were examined. This effectively corresponds to varying the power of the reflected wave. Consequently, from the following section onward, the BER characteristics are examined using the power of the direct wave and the power of the reflected wave as parameters.

4.3. BER characteristics relative to the ratio of direct wave power and reflected wave power

In Section 4.2, the BER characteristics relative to changes in the reflection coefficient (strength of reflected wave) are shown, but here, in order to further clarify the relationship between the direct wave and reflected wave, the BER characteristics are examined for the case where the powers of the direct wave and the reflected wave (total in the case of two or more waves) are P_D and P_R respectively and P_R/P_D is varied as follows: –6 dB, –10 dB, –15 dB, –20 dB. Figure 12 shows the BER characteristics in the cases of 5-, 10-, and 20-symbol delays and P_R/P_D is varied. In the case of the 5-symbol delay in Fig. 12(a), the BER has an error floor occurring before 10^{-1} and 10^{-2} respectively at P_R/P_D = –6 dB, –10 dB, and practical communication is difficult in the region where P_R/P_D is greater than –10 dB. In the case of the 10-symbol delay in Fig. 12(b), a floor occurs near where the BER drops below 10^{-2} only when P_R/P_D = –6 dB. Otherwise there is no large floor and actual communications are possible without any problems. In the case of the 20-symbol delay in Fig. 12(c), the same trends appear as in the case of a 10-symbol delay [Fig. 12(b)]. When Fig. 12 is taken as a whole, communication is possible if P_R/P_D is smaller than –15 dB, even if there is a reflected wave.

When the number of delay symbols varies in Fig. 12, the BER characteristics are seen to change slightly, though this is not the influence of P_R/P_D. In particular, the charac-

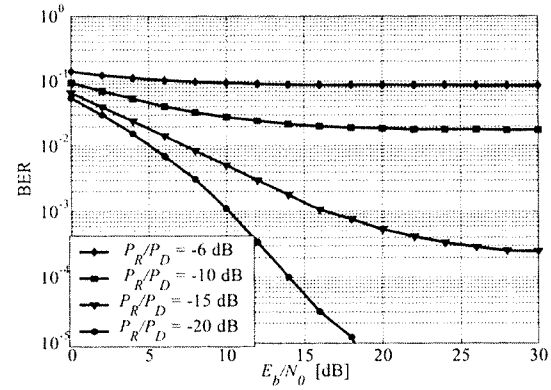

(a) 5-symbol delay

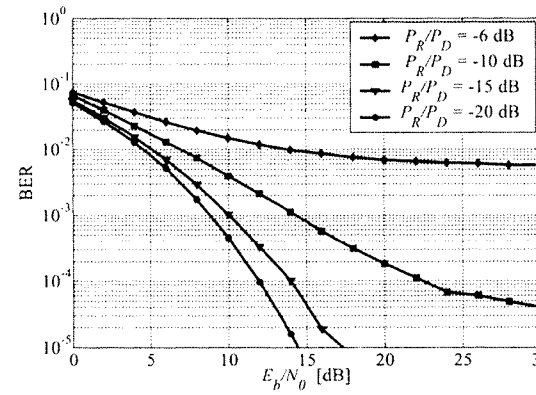

(b) 10-symbol delay

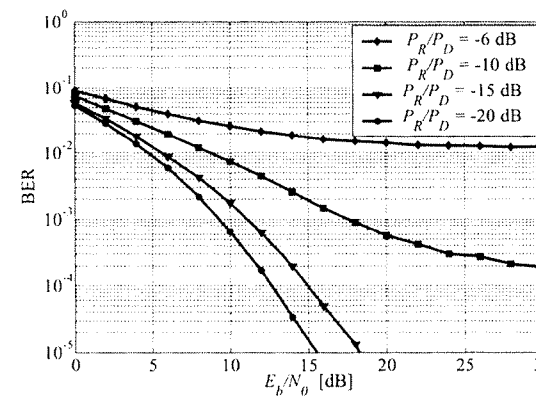

(c) 20-symbol delay

Fig. 12. BER characteristics for P_R/P_D.

teristics become the worst in the case of the 5-symbol delay. Thus, to learn whether the BER also becomes correspondingly poor when the symbol delay becomes smaller than that, the BER characteristics were examined for varying symbol delays with E_b/N_0 held constant at 10 and 20 dB. Figure 13 shows the results; it is seen that the BER does not deteriorate as the symbol delay becomes smaller, while there are also cases when the BER deteriorates when the symbol delay is large (for example, the 2- and 8-symbol delays in Fig. 13). In other words, the BER is thought to change successively with the influence of the waveform distortion from the addition of the reflected wave. However, the amount of that change is dominated by P_R/P_D when the influence of P_R/P_D is great overall.

4.4. BER characteristics for varying numbers of paths

The two-wave model has been discussed up to now, but here the characteristics are examined for varying path numbers, meaning an increased number of paths for the reflected wave. Figure 14(a) shows the BER characteristics for a three-path system, meaning a direct wave and two reflected waves. Here the number of delay symbols is set in consideration of the similar results obtained in Figs. 12(b) and 12(c). The first reflected wave has a 10-symbol delay and the second has a 20-symbol delay so that the average number of delay symbols becomes 15 symbols. Also, the first and second reflected waves have the same power. The results in Fig. 14(a) display the same trends as those in Fig. 12. If P_R/P_D is less than –15 dB, it can be determined that wireless transmission is possible even without the addition of equalization and error correction technology. Figures 14(b) and 14(c) show the BER characteristics for four- and five-path systems under the same conditions as the three-path system. The four-path case had reflected waves arriving with 10-, 15-, and 20-symbol delays; the five-path case had reflected waves arriving with 5-, 10-, 20-, and 25-symbol delays; and the reflected waves had the same power. The results in Fig. 14 indicate that the characteristics deteriorate little by little, even with the same P_R/P_D when the number of paths is increased. This is believed to be caused by the level of waveform distortion due to the addition of many

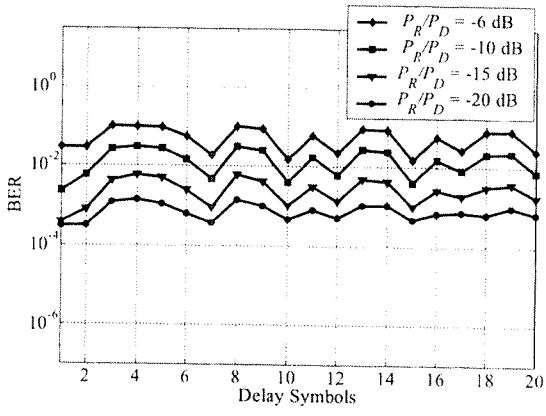

Fig. 13. BER characteristics with varying the number of delay symbols (E_b/N_0 = 10 dB).

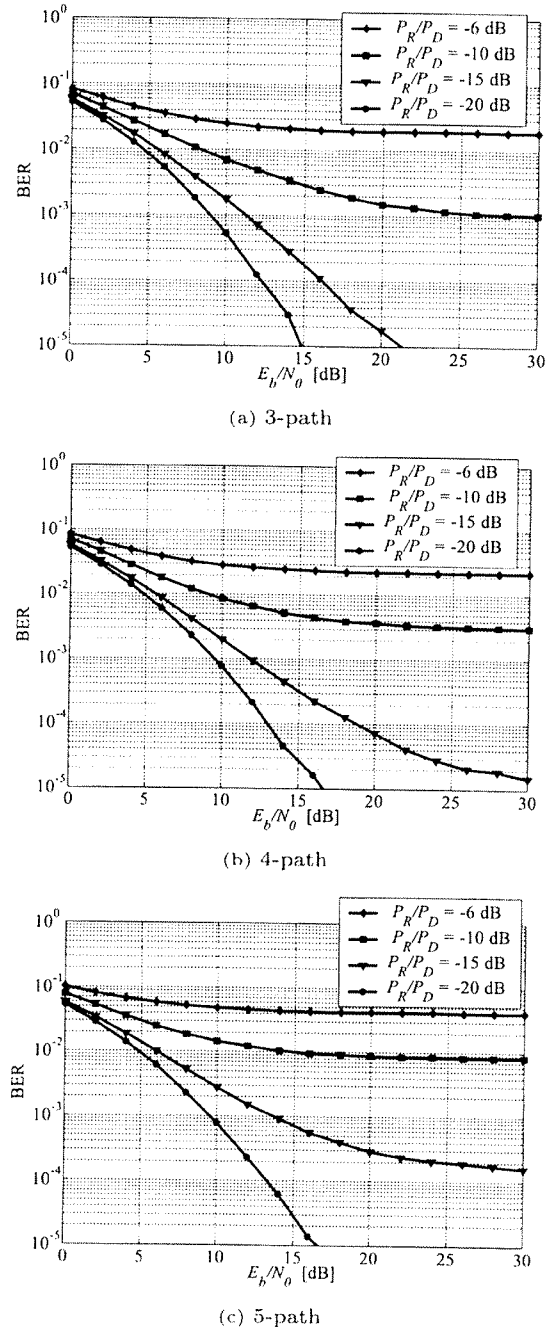

Fig. 14. BER characteristics for 3-, 4-, and 5-path systems.

reflected waves. However, the overall trend is that the portion depending on P_R/P_D is greater than the number of paths, and particularly when P_R/P_D is –20 dB, the same BER characteristics are obtained with three-, four-, and five-path systems.

4.5. Discussion

Sections 4.1 to 4.4 are considered here. In the case of free space, wireless baseband transmission had results of less than 3 dB at a BER of 10^{-4}, compared to BPSK. In a multipath environment, the combination of equalization and error correcting technology are believed to be necessary in an environment of strong reflected waves such that P_R/P_D is greater than –10 dB. However, in a relatively weak multipath environment where P_R/P_D is less than –15 dB, practical communication is possible even without combining those technologies. From the results of varying the number of paths of the reflected waves in Section 4.4, it is understood that P_R/P_D has a greater influence on the BER characteristics than the number of paths. In other words, in an environment with many reflected waves, this is not problematic for the BER if the total P_R is less than the P_D (–20 dB, for example). Oppositely, even with only one reflected wave, there is a large influence on the BER if that reflected wave is only damped by 6 dB compared to the direct wave. In such an environment, the combination of equalization and error correcting technologies is desirable.

As an example of equalization, Fig. 15 shows the results in the case where the channel characteristics of Fig. 8(b) are equalized over a range of 700 MHz to 2 GHz. The equalization range finds the optimum values through simulation. Figure 15 indicates that, even where the floor occurs at a BER of 10^{-3} before equalization [same as multipath (actual) in Fig. 10], equalization improves the BER to less than 10^{-4} with E_b/N_0 being 12 dB and that equalization operates effectively in wireless baseband transmission as well.

This section contains a discussion of an arbitrary multipath environment discussed in Section 2.3.2 drawn from the channel characteristics (values measured with the VNA) in free space. Section 2.3.1 shows that in the case of one path (free space), the directly measured values in the

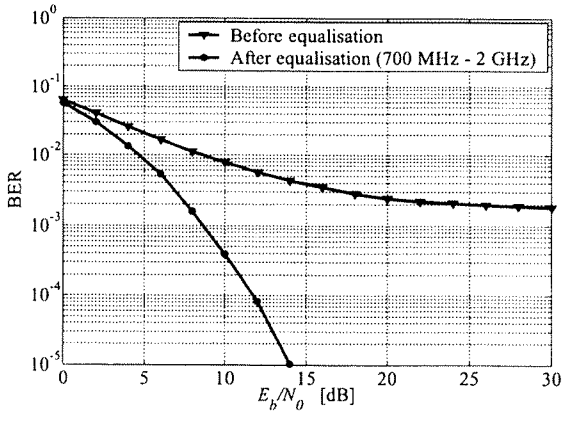

Fig. 15. BER characteristics before and after equalization.

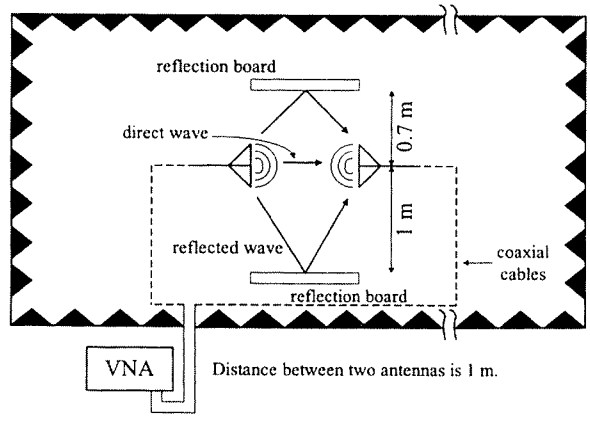

(a) Environment

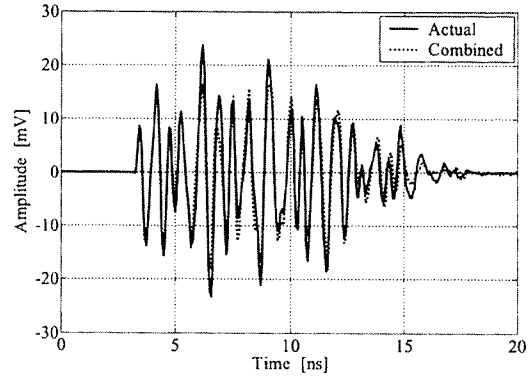

(b) Received waveforms

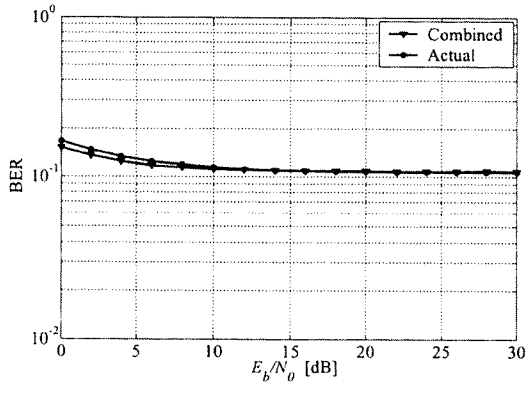

(c) Received waveform

Fig. 16. Received waveforms and BER characteristics for 3-path.

time domain and measured values in the frequency domain are input to a computer and processed, then returned to the time domain where the characteristics match. In Section 2.3.2, in the case of a two-path system (direct wave + reflected wave) based thereon, it is discussed how the characteristics match for a reflection board disposed in a real system and those of an environment modeled on a computer using only the free space channel characteristics. In this paper, the system is treated as linear as discussed in Section 2.1 and therefore, the same type of conclusion is derived in the case of increasing the number of paths to three, four, and five paths as in Section 4.4. Finally, to confirm this for the three-path system, the characteristics in the case of establishing two reflection boards [Fig. 16(a)] and characteristics in the case of a computer model of that environment based on the channel characteristics of free space only are shown in Fig. 16. The measurement conditions are the same as those discussed in Section 3. As in the two-path cases in Figs. 4 and 10, results which are nearly the same for both are obtained from Fig. 16. In Fig. 16(c), the BER reaches the floor before reaching 10^{-1}. In this case, when regarded in the same manner as Eq. (5), this is the arrival of a reflected wave with an amplitude of 0.58 [reflected by the reflection board at a distance of 0.7 m in Fig. 16(a)], and a reflected wave with an amplitude of 0.45 [reflected by the reflection board at a distance of 1 m in Fig. 16(a)]. Specifically, this is the following equation and τ_1 and τ_2 are 2.4 and 4.0 ns, respectively:

$$y(t) = x(t) - 0.58x(t - \tau_1) - 0.45x(t - \tau_2) \quad (7)$$

P_R/P_D at this time is approximately –3 dB. This is a harsher environment than the case of P_R/P_D = –6 dB in Fig. 14(a); the BER floor value deteriorates from just short of 10^{-2} to almost 10^{-1}. This also indicates the validity of the results. Accordingly, the same results as in the two-path case are obtained in the three-path case as well. It can be determined that the same type of results are obtained when the number of paths is increased to four and five. Moreover, there is no problem even when a multipath environment was modeled on a computer and evaluated.

5. Conclusions

A real-valued signal analysis method for wireless baseband transmission was shown. Using this method, the BER characteristics in a multipath environment were found using measured channel characteristics. In an evaluation through a partial simulation, it was found that 2.5-Gbit/s transmission could be implemented with a 10-cm square antenna. Regarding transmission characteristics of wireless baseband transmission in a multipath environment, it was found that, if the ratio of direct wave power to reflected wave power P_R/P_D was made smaller than –15 dB, then it was possible to have practical wireless transmission where the BER was 10^{-4} or less without integrating equalization and error correcting technologies. Also, the BER was clearly dominated by P_R/P_D rather than the number of paths. Under a stronger multipath environment, it was found that sufficient performance could not be obtained due to code interference, and therefore future research into multipath countermeasures such as equalizer technology or the like is necessary.

REFERENCES

1. Kitagawa J, Taniguchi T, Karasawa Y. Wireless baseband transmission experiments. IEICE Trans Commun 2006;E89-B:1815–1824.
2. Komiyama B. Introduction to the contents of research at ATR Adaptive Communications Research Laboratories. ATR J 1996;23:7–10.
3. Kobayashi T, Kouya S. Overview of research and development in ultra wideband systems. IEICE Trans 2003;J86-A:1264–1273.
4. Kohno R. Collaboration among industry, academia and government for R&D of the ultra wideband wireless technologies and contribution in standardization in wireless PAN. IEICE Trans 2003;J86-A:1274–1283.
5. Maeda T. UWB antennas technology: Antenna and propagation technologies for ubiquitous ultra high speed wireless communications and perspectives. IEICE Trans 2005;J88-B:1586–1600.
6. Aiello GR, Rogerson GD. Ultra-wideband wireless systems. IEEE Microwave Mag 2003;4:36–47.
7. Porcino D, Hirt W. Ultra-wideband radio technology: Potential and challenges ahead. IEEE Commun Mag 2003;41:66–74.
8. Karasawa Y. Fundamentals of wave propagation for digital mobile communications. Corona; 2003.
9. Molisch AF. Ultrawideband propagation channels—theory, measurement, and modeling. IEEE Trans Veh Technol 2005;54:2087–2104.

AUTHORS (from left to right)

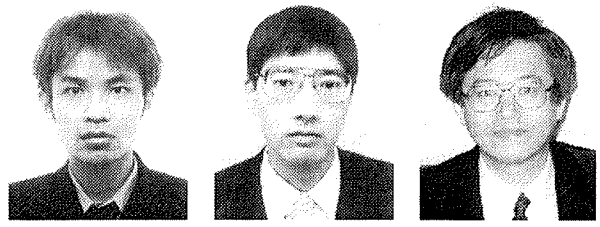

Jun-ichi Kitagawa (student member) received a bachelor's degree in Interdisciplinary Science and Engineering from Shimane University in 2001 and M.E. and Ph.D. degrees from the University of Electro-Communications in 2003 and 2006. In 2007, he joined Yuitech Corporation Limited as a radio frequency engineer. He is a First-Class Radio Operator for General Services and a First-Class Technical Radio Operator for On-the-Ground Services.

Tetsuki Taniguchi (active member) received his B.S. and M.S. degrees in electrical engineering from Tokyo Metropolitan University in 1989 and 1991 and D.Eng. degree in natural science from Kanazawa University in 1996. In 1992, he joined Kanazawa University, where he worked as a research assistant in the Department of Electrical and Information Engineering, and a researcher at MAGCAP (Laboratory of Magnetic Field Control and Applications). In 2001, he joined the University of Electro-Communications, where he is currently a research assistant in the Department of Electronic Engineering. His research interests are in digital signal processing, digital communications, and nondestructive evaluation. He is a member of IEEE, the Institute of Electrical Engineers of Japan, and the Japan Society of Applied Electromagnetics and Mechanics.

Yoshio Karasawa (active member) received his B.E. degree from Yamanashi University in 1973 and M.S. and D.Eng. degrees from Kyoto University in 1977 and 1992. He joined KDD R&D Labs. in 1977. From 1993 to 1997, he was a Department Head of ATR Optical and Radio Communications Research Labs. and ATR Adaptive Communications Research Labs. Currently, he is a professor at the University of Electro-Communications. Since 1977, he has engaged in studies on wave propagation and antennas, particularly on theoretical analysis and measurements for wave-propagation phenomena, such as multipath fading in mobile radio systems, tropospheric and ionospheric scintillation, and rain attenuation. His recent interests are in frontier regions bridging "wave propagation" and "digital transmission characteristics" in wideband mobile radio systems such as MIMO. He received the Young Engineer Award from IECE of Japan in 1983, the Meritorious Award on Radio from the Association of Radio Industries and Businesses in 1998, Research Award from ICF in 2006, and two Paper Awards from IEICE in 2006. He is a senior member of IEEE and a member of SICE Japan.